ELSEVIER

Fuzzy Sets and Systems 69 (1995) 15–27

FUZZY sets and systems

# Fuzzy logic and autonomous vehicles: Experiments in ultrasonic vision

M. Poloni*, G. Ulivi, M. Vendittelli

*Dipartimento di Informatica e Sistemistica, Università degli Studi di Roma "La Sapienza", Italy*

Received September 1993; revised March 1994

**Abstract**

The opportunities offered by fuzzy logic to build maps for robot navigation are investigated. Characteristics of points of the space (occupied, free, uncertain, etc.) are easily expressed through set theoretical operations. Real-world experiments validate the approach. The experimental set-up is based on modified Polaroid ultrasonic sensors; however, the approach can be easily extended to incorporate other kinds of sensors.

*Keywords:* Data analysis methods; Linguistic modeling; Robotics

## 1. Introduction

Use of mobile robots is spreading in many fields of application. Typical examples are submarine and spatial exploration [21, 11, 9], surveillance of industrial installations, rescue missions in dangerous environments (radiations, chemical contamination). More common applications are, for example, internal mail delivery, partially autonomous wheel-chairs for disabled [20], intelligent Automatic Guidance Vehicles (AGVs) for floor-shops [2].

Despite the differences among these applications, an autonomous vehicle always needs a navigation system to determine a suitable path to its target and a sensory system to acquire knowledge about the crossed environment.

Consider the simplified functional structure of a navigation system depicted in Fig. 1. At the beginning the map can be totally or partially unknown. The lowest level is constituted by the measuring processes that supply rough information coming from each sensor, typically the distance of the nearest obstacle (Sensors). Information is suitably merged and used to build or upgrade the map of the traveled environment (Map reconstruction). The map is used to implement the navigation strategy. It can also be interpreted by other levels of the structure, trying to identify the shape and possibly the nature of the objects on the scene (Map interpretation) to devise more complex strategies [18]. In this case the map could contain other details on the environment as, for example, the colors of the obstacles.

* Corresponding author. Correspondence address: ELITE Foundation, Promenade 9, 52076 Aachen, Germany.


*SSDI* 0165-0114(94)00237-1

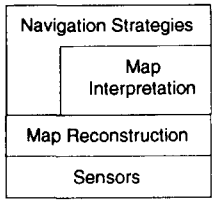


Fig. 1. Structure of a navigation system.

When full autonomy is pursued in a highly unstructured environment, sophisticated sensors are typically used, e.g. video cameras; however, this solution requires an expensive hardware and a complex software.

In simpler applications the environment can be assumed planar and some a priori knowledge on the obstacle nature is available, typically that they are prismatic. In these cases, ultrasonic (US) sensors are often used as they are cheap, light and reliable.

Beside these positive characteristics, US sensors show also two main drawbacks. First, the wide angle of radiation causes large uncertainties on the angular location of the obstacle that originates the echo. Second, the ultrasonic beam is easily reflected when it hits a surface with a large angle of incidence. After some reflections it can find a path to return back to the sensor or it can go lost. Therefore, the measured distance can be quite longer than the one of the nearest object.

A well-known application of ultrasonic sensors in this area is described in [5] where the uncertainties have been managed in a stochastic setting.

Stochastic methodologies [6, 4] can produce reliable results from uncertain readings when a high number of data is available and they are well distributed in the explored area. In this case averaging can reduce the overall uncertainty shown by the final map. Clearly, with a limited number of measures the results are not so good; indeed, further studies have been carried out to improve the efficiency of map building. In [7] the angle of incidence is estimated to derive the probability of a multiple reflection, in [12] typical environment configurations (e.g. corners) are classified and used to improve the map accuracy.

A different approach to uncertainty handling is provided by the theory of fuzzy sets, which allows a great flexibility in the treatment of information (see e.g. [10, 23, 1]). This theory has already been used in the field of navigation of mobile robots [13, 18], especially in the highest layers of the navigation structure scene interpretation (particularly for scenes derived by cameras) and path planning have been extensively studied (see [14, 15, 8]).

This paper is an exploration of the possibilities offered by this theory for map reconstruction from sonar data but other kinds of range finders can be considered simply modifying the description of the uncertainties they introduce, namely the sensor uncertainty model.

After a brief introduction of the used notations and operators, the sensor characteristics are outlined and an uncertainty model derived. As in [5], measures are used to build two maps. The first concerns the free areas, the other the occupied ones. Both maps specify our degree of belief about the status of each point of the space. Fuzzy logic is used to give a formal description of the manipulations of the maps; this allows to carry out several characteristics of the environment. The operations are described in natural language and easily formulated using fuzzy set operators. A description of the experimental set-up and of the obtained results conclude the paper.

## 2. Notations and operators

Given a crisp universal set $U$ and denoting by $u$ its generic element, a fuzzy set $A \subseteq U$ will be identified by its membership function:

$$A(u): U \to [0, 1].$$

In the paper, rectangular bidimensional maps are considered. Therefore, the universal set and its elements are, respectively, specified as $U = X \times Y$ and $u = (x, y)$, being $x$ and $y$ the Cartesian coordinates of a point in the map and $X$ and $Y$ their ranges.

Each point can be either empty or occupied, 'a crisp property. However, because of the measuring uncertainties, we can express only a degree of belief about these properties. As explained later, two fuzzy sets are used to express "emptiness" and "fullness":

$$E(x, y): X \times Y \to [0, 1], \qquad O(x, y): X \times Y \to [0, 1].$$

Several logical operations are defined for these fuzzy sets by trivial extension of the unidimensional ones.

The set complementation is implemented, as usual, by

$$c(A(u)) = 1 - A(u). \tag{1}$$

As for the intersection, both the algebraic product

$$i(A(u), B(u)) = A(u) \cap B(u) = A(u) * B(u) \tag{2}$$

and the bounded product

$$i(A(u), B(u)) = A(u) \cap B(u) = \max(0, A(u) + B(u) - 1) \tag{3}$$

are used.

By De Morgan law, set union is defined, respectively, as the algebraic sum:

$$u(A(u), B(u)) = A(u) \cup B(u) = A(u) + B(u) - A(u) * B(u) \tag{4}$$

and the bounded sum

$$u(A(u), B(u)) = A(u) \cup B(u) = \min(1, A(u) + B(u)). \tag{5}$$

In the following, we shall refer to the couples (2, 4) and (3, 5), respectively, as AP and BS couples.

In this paper also parameterized union operators has been considered, due, respectively, to Dombi and Yager [3, 10, 22]:

$$\frac{1}{1 + \left[ \left( \frac{1}{A(u)} - 1 \right)^{-\lambda} + \left( \frac{1}{B(u)} - 1 \right)^{-\lambda} \right]^{-1/\lambda}} \tag{6}$$

for $\lambda \in (0, \infty)$ and

$$\min\left[ 1, \sqrt[p]{A(u)^p + B(u)^p} \right] \tag{7}$$

with $p > 0$.

## 3. Sensor modeling and map building

Generally an ultrasonic sensor is composed by two fundamental elements: the acoustic transducer and a ranging circuit board. It works in a simple way: a packet of ultrasonic waves is generated and the resulting echo is detected. The time between the transmission and the reception of the packet is proportional to the distance of the obstacle. More sophisticated techniques could be used, including real-time signal processing; however, this would require expensive computation devices.

We assume a typical office-like environment, occupied by prismatic obstacles extending indefinitely in the vertical direction. Therefore, the points of an ideal map are either empty or occupied.

The measuring process, however, introduces several kinds of uncertainties, mainly related to the characteristics of the used sensor. One source of uncertainty is given by the non-zero width of the radiation cone (about 30° for the used ones), making it impossible to know exactly the angular position of the object which originated the echo; for example the first three cases in Fig. 2 all give the same result. Moreover, the beam may go easily lost or it may be reflected more than once before coming back to the sensor as shown by the last case in the same figure. As a consequence, each point of the real map can be assumed empty or occupied with a certain degree of belief and the two conditions are not mutually exclusive. Very low degrees of belief for both attributes in a point denote a lacking of information, while two very high values imply a contradiction due, e.g. to a poor accuracy of the measures.

In the process of map building several bidimensional fuzzy sets are determined by iteratively mapping the sensor model on the grid. Indeed, the final map itself results to be a fuzzy set. All these are defined over a bidimensional universal set corresponding, in our experiments, to a square with 10 m sides. For computational reasons, the square is subdivided in $100 \times 100$ square cells. This approach is well suited to describe by simple linguistic statements the operations necessary to derive a navigation map and moreover its grid-based nature complies with the implementation of path planning algorithms.

The choice of a suitable sensor model (more exactly: of the whole sensor-environment interaction) is of paramount importance for the overall performance. It should describe all the phenomena involved in the measuring process. In the authors' opinion, a precise numeric approach – e.g. based on an accurate analysis of the shape of the radiation lobe – is useless because of the level of the overall uncertainty. Here only qualitative (linguistic) descriptions of the different phenomena are used and expressed in terms of simple functions.

a. Neglecting beam reflections, a single measure provides the information that one or more obstacles are located somewhere on the 30° arc of circumference of radius $r$ (the measured distance). Hence, there is a possibility for each of the cells "near" the arc to belong to the set $\omega$ of the occupied ones. A simple parabola models this phenomenon:

$$g_a(\rho) = \begin{cases} \left[1 - \left(\dfrac{\rho - r}{\Delta\rho}\right)^2\right] & \forall\rho\colon |\rho - r| < \Delta\rho, \\ 0 & \text{otherwise,} \end{cases} \tag{8}$$

where $r$ is the distance measured by the US sensor, with a range between 0.3 and 8 m, $\rho$ is the radial distance of the cell from the sensor, and $\Delta\rho$ is an estimate of the overall accuracy. Among the factors contributing to the fuzziness of the concept of "near" are the errors affecting the measures and the map discretization, i.e. the sensor and the obstacle(s) are generally located off the cell centers.

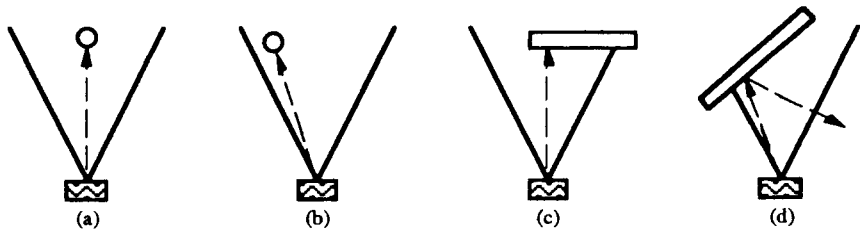


Fig. 2. Typical uncertainties with ultrasonic sensors.

Two remarks are in order: (a) the sum of the occupation possibilities of the cells near the arc is not equal to one because one or more cells may be occupied; (b) the repetition of the same measure can reduce only a little the overall uncertainty which mainly depends on non-stochastic factors.

b. Cells inside the circular sector of radius $r$ show an evidence to be free from obstacles, so they belong to the set $\varepsilon$ of the empty cells. This is simply expressed by

$$g_b(\rho) = \begin{cases} 1 & \forall \rho < r - \Delta\rho, \\ 0 & \text{otherwise.} \end{cases} \tag{9}$$

c. Reflections modify our belief about the status of the explored cells. As reflected beams make a longer fly than direct ones, the simplest way to tackle with this phenomenon is to gradually reduce our belief from a maximum to a minimum according to the distance $\rho$:

$$g_c(\rho) = \min(1, h_1 e^{-h_2\rho} + h_3). \tag{10}$$

Parameter $h_3$ represents the minimum degree of belief, $h_1, h_2$ are used to interpolate between the two values and take into account average distances in the environment.

d. The wave intensity decreases far from the beam axis and reaches zero at the borders of the lobe. Therefore, the belief of each assertion is higher for the cells nearer to the beam axis. The cells outside the lobe do not change their attributes.

$$g_d(\vartheta) = \begin{cases} 1 - (\frac{12}{\pi}\vartheta)^2 & \forall \vartheta\colon |\vartheta| < \pi/12, \\ 0 & \text{otherwise.} \end{cases} \tag{11}$$

e. Even in ideal situation a single measure is not sufficient to gain certainty on the status of a cell. Indeed each cell is to be "viewed" several times and its occupancy and emptiness result from the union of many measures. The weight of the elementary acquisition is given by two coefficients: $k_\varepsilon$ and $k_\omega$, respectively, for emptiness and occupancy.

With the used sensors, the values of the parameters are, respectively: $\Delta\rho = 0.15$, $k_\omega = 0.5$, $k_\varepsilon = 0.1$, $h_1 = 1.2$, $h_2 = 1$, $h_3 = 0.1$.

Given a cell located at a distance $\rho$ from the range finder and an angle $\theta$ from its axis, its possibilities to be empty or occupied are obtained by adding the previous values.[1] For computational reasons, the algebraic product is used, however, it could be substituted by other operators:

$$\varepsilon'(\theta, \rho) = k_\varepsilon g_b g_c g_d, \tag{12}$$

$$\omega'(\theta, \rho) = k_\omega g_a g_c g_d. \tag{13}$$

The prime denotes that these membership functions are referred to polar coordinates, the same way they are represented (normalized) in Fig. 3 in the sample case of a measured distance equal to 2.9 m.

To build the map several measures are taken from known points in the considered environment. Here we will neglect the way the robot reaches these points. However, as it will become clear in the sequel, the map can be reconstructed step by step, as the robot moves among the free cells.

For each reading $k$ the two surfaces $\varepsilon'(\theta, \rho)$ and $\omega'(\theta, \rho)$ are projected on the cells of the Cartesian map using a recursive algorithm whose complexity is linear in the number of interested cells. The outputs of the projections are two fuzzy sets $\varepsilon_k(i,j)$ and $\omega_k(i,j)$, being $i, j$ the indices of the cell matrix.

[1] These functions are used to generate a fuzzy set from a measure. This "fuzzification stage" is quite different from that generally used in fuzzy control.

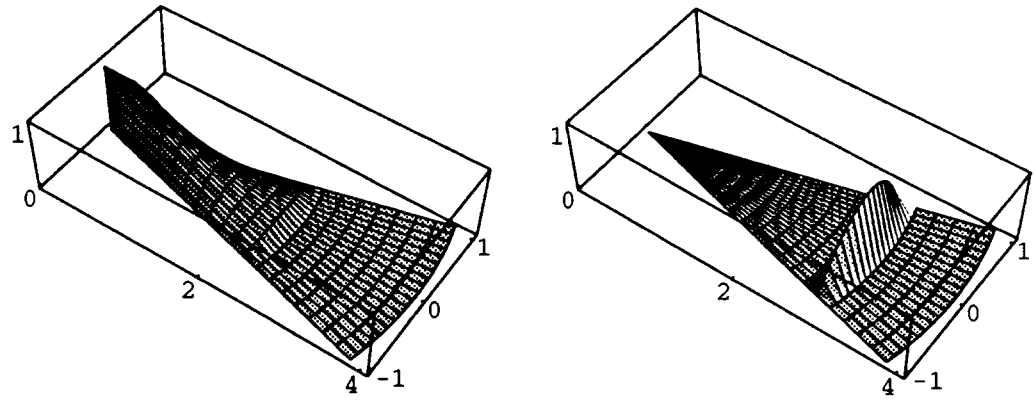


Fig. 3. Sensor certainties for empty (left) and occupied cells (right) in a typical case.

The pieces of information concerning the empty and the occupied cells are separately collected during the measuring process using a union operator. The associative property of these operators allows using two fuzzy sets $E(i,j)$ and $O(i,j)$ as accumulators. As a consequence the procedure can be used also while the robot is moving. At the end of the process the two sets assume the values:

$$E(i,j) = \bigcup \varepsilon_k(i,j), \tag{14}$$

$$O(i,j) = \bigcup \omega_k(i,j), \tag{15}$$

being the union performed over all the available measures. For this operation Dombi's union (6) has been used. In fact the max operator is not suitable in this context as it does not allow to the final belief to "sum up" all the available information. Other operators (e.g. Yager ones (7)) "saturate", i.e. they give formal certainty after a certain number of concordant measures. The chosen union family only asymptotically reaches certainty; in this sense it is more appropriate for our purposes. Figs. 4 and 5 refer a simple comparison: they show how the degree of belief increases for a given cell in the case that the measures continuously give a certainty equal to 0.1. With the chosen values for parameters $p$ and $\lambda$ the two families of curves show similar values for a small number of measures.

Interesting comparisons among these and other parametric union operators can be found in [19, 22].

The two obtained sets (maps) of the *empty* cells and of the *occupied* ones can be combined in several ways (from now on, the linguistic attributes which assume a formal meaning will be slanted). Their intersection, for example, represents the set of cells for which the measures are *ambiguous*, with the membership values giving a degree of contradiction:

$$C(i,j) = E(i,j) \cap O(i,j). \tag{16}$$

The set of the *unexplored* cells can be obtained as

$$Q(i,j) = \bar{E}(i,j) \cap \bar{O}(i,j), \tag{17}$$

where the overbar indicates set complementation.

The kind of elaboration depends on the application. If the main task of the robot is to build an accurate map, then the contradictory cells should be explored first. For navigation purposes, what is needed is a conservative map of the *free* cells $M(i,j)$. Accordingly, this map can be built by "subtracting" the *ambiguous* cells from the *empty* ones:

$$M(i,j) = E(i,j) \cap \bar{C}(i,j), \tag{18}$$

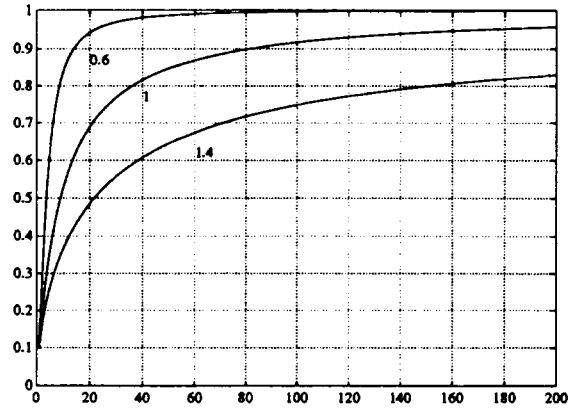


Fig. 4. Certainty accumulation according to Dombi union (certainty vs. iterations).

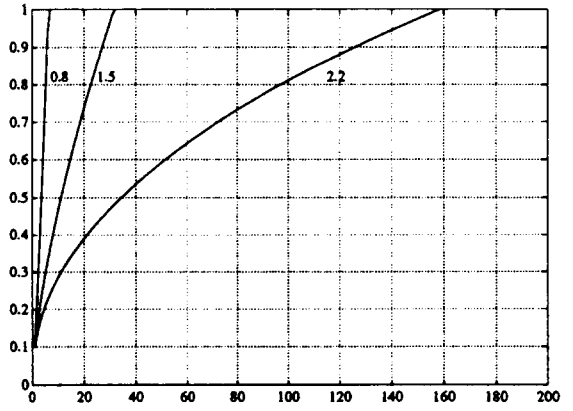


Fig. 5. Certainty accumulation according to Yager union (certainty vs. iterations).

A more conservative map can be obtained getting rid also of the *occupied* cells. Formally, this can be expressed as

$$M(i,j) = E(i,j) \cap \bar{O}(i,j) \cap \bar{C}(i,j). \tag{19}$$

The results obtained with these two formulations have been compared in the next section. As for the set theoretical operations, both the couple of equations (2), (4) and (3), (5) have been used.

## 4. Experimental set-up

The used ultrasonic sensor is a commercial device from Polaroid Corporation [16, 17]. It is composed of two fundamental elements: the acoustic transducer with the associated analog electronics and a ranging circuit board.

The device emits a chirp signal of 1 ms duration, made of 56 pulses at a frequency of 49.41 kHz. The main rediation lobe covers a solid angle of about 30° at − 38 dB.

The standard Polaroid's ranging system is able to detect the presence of objects in a range from 30 cm to 10 m.

To obtain better performances a new ranging circuit has been designed, which is able to drive eight sensors. Note, however, that only one sensor at a time can be fired to avoid cross-interference problems.

Using the suggestions given in [16], the minimum range has been lowered to 10 cm and it is possible now to select two different types of resolution: high ($\approx$ 1 cm) and low (4.5 cm). At high resolution, the maximum distance that can be measured is about 60 cm.

The board has been interfaced to a Hewlett Packard 16 MHz VECTRA 386SX computer by means of a Burr-Brown 32 bit parallel communication card. Data exchange is based on a 16 bit bus: one byte is for board control, while the other contains the numerical data proportional to the distance covered by the acoustic wave. The eight bits of control are configured as follows: three are for the addresses of the ultrasonic sensors, three are for coordination with other sensory systems or for future board capabilities, two gives, respectively, the start signal for the US pulse and the desired resolution (high/low).

The PC selects and fires the sensors, collects the results and elaborates the maps by means of the algorithms defined in the following. A sketch of the experimental set-up is given in Fig. 6.

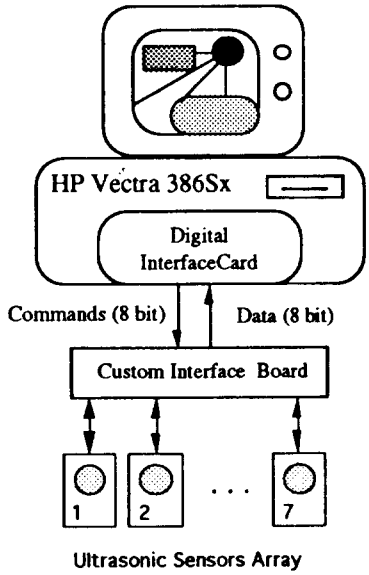


Fig. 6. Experimental set-up.

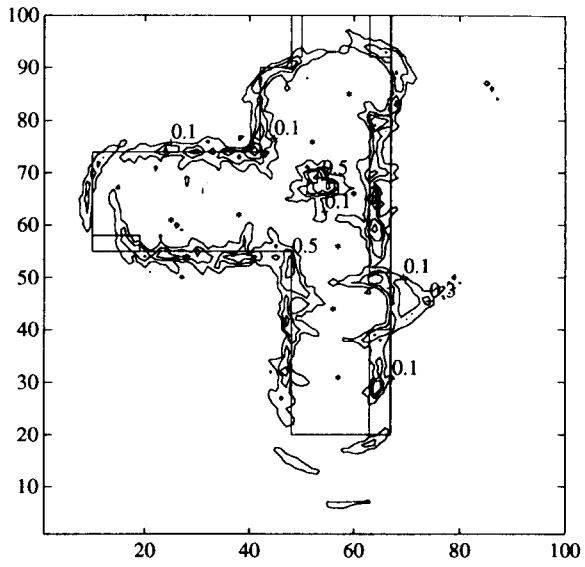


Fig. 7. Map of the occupied cells.

In the presented experiments only one sensor is used, which is rotated 9° at each measure until a 360° scan is performed. Larger steps have been tried, but they gave worse results. The sensor is mounted on a trolley at 1.3 m above the floor. Each measure takes about 0.25 s. Several independent readings from the same position are averaged to reduce the effects of the transducer sensitivity fluctuations.

All the software is implemented in C language. The main functions include the low-level sensor interfaces, the projection of $\varepsilon'(\theta, \rho)$ and $\omega'(\theta, \rho)$ on the Cartesian frame, the accumulation according to (14), (15), and finally the map building. The execution of the whole program for eight measuring points last about 1.25 s on the aforesaid machine.

## 5. Experimental results

The described map building system has been tested in a corridor of our department. This is rather long and narrow, with several book cabinets located by the walls, so that beams are easily reflected. Halfway the corridor there is a widening where a slim irregular obstacle has been added. The ultrasonic sensor has been manually placed in eight known locations and 40 measures have been taken from each of them to cover the whole circle. The chosen test-environment is coherent with our research goal, i.e. a mobile robot capable of reconstructing and navigating in an unknown office-like environment. It emphasizes the issues of reflection, reconstruction of convex and concave corners and of the resolution of narrow walk-through passages that can be hidden from the arc-shaped response of the sensor. In the following the maps are represented by contour plots; the level lines are generally drawn at 0.3, 0.5 and 0.7. No scaling or normalization has been applied during data processing.

The overall maps of the *occupied* and of the *empty* cells are given, respectively, in the contour plots of Figs. 7 and 8. Using a value 0.6 of $\lambda$ in the Dombi's union, the values of the membership functions of the two maps range, respectively, between 0 and 0.85 and between 0 and 0.88. The actual map of the corridor and of the obstacle is superimposed to the plots and the locations of the points of measure are marked with asterisks.

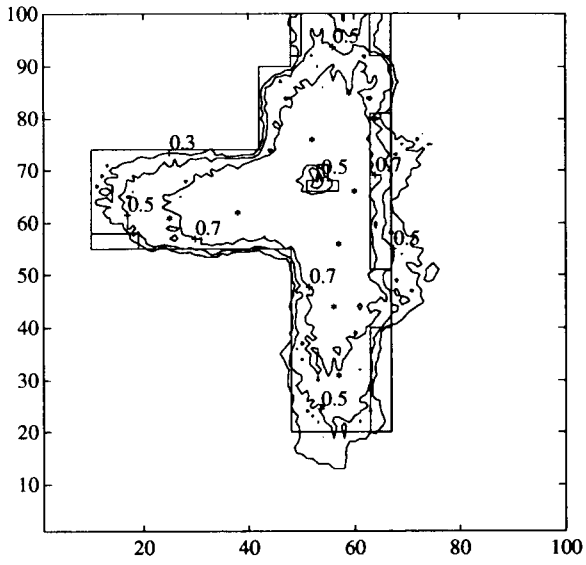


Fig. 8. Map of the empty cells.

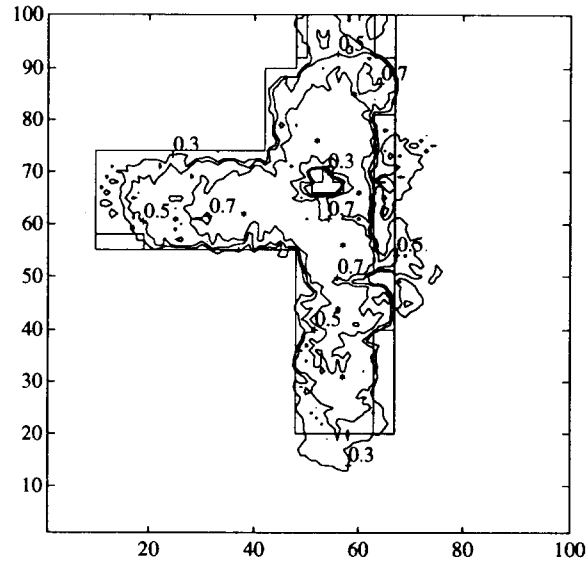


Fig. 9. Map from Eq. (19) and BS operators.

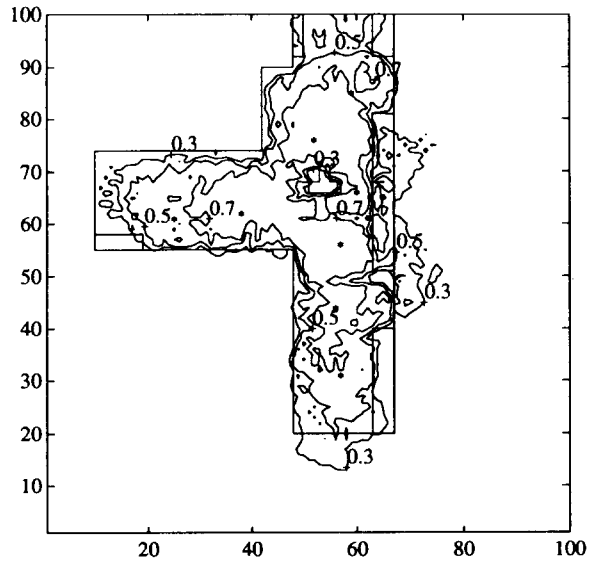


Fig. 10. Map from Eq. (19) and AP operators.

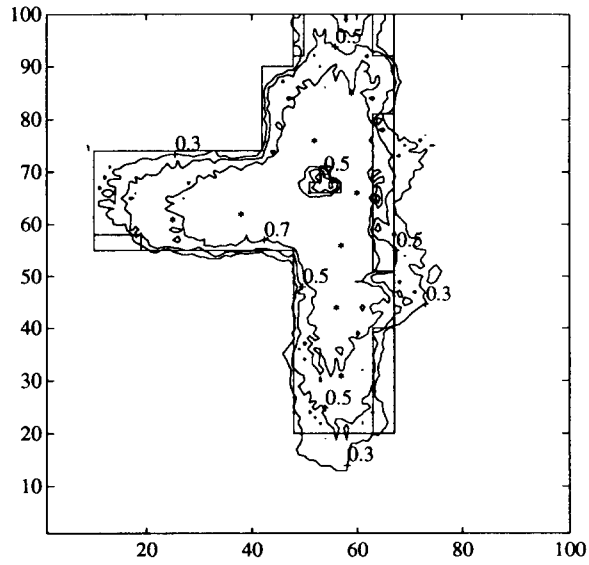


Fig. 11. Map from Eq. (18) and BS operators.

The first of the two maps is cluttered by many beam spurious reflections, revealed by missed walls (e.g. in 45–65, 20–30). The effect of the lobe width is evident near the corners where arc shaped artifacts appear (e.g. 55–80, 40–50). To make these phenomena more evident a contour line at 0.1 has been added. The map of the empty cells is compact and seems a good representation of the corridor. However, note that even the contour line 0.7, which encloses an area (almost) certainly free, in (65, 50–80) is behind the actual wall.

Moreover, the large distance among the contour lines denote a lack of resolution. This is one of the main "quality indices" considered in the following, the other one being obviously the reliability of the navigation map.

We tested the four combinations obtained implementing Eqs. (18) and (19) by both AP and BS operators. All the combinations give good results especially considering the small number of measures. Note that all the maps range between 0 and 0.88.

The best results have been obtained using Eq. (19) and the BS couple of operators. The resulting map is given in Fig. 9. It can be compared with Fig. 10, obtained by the same equation but using the AP couple. Note in the former map the sharpness of the detected walls in particular on the right side of the corridor, also the doors between the book cabinets are well drawn. The contour line at 0.5 is always contained in the safe zone, except for a small area near the point (65, 52).

In the latter map the level lines are generally more distant and the obstacle results quite larger than in the previous map and is almost connected to the wall.

The (small) improvements of the BS couple over the AP one, can be attributed to the different strength of the two implementations of the intersection:

$$i_{BS}(a,b) \leqslant i_{AP}(a,b) \quad \forall a,b.$$

Worse results are produced by Eq. (18) with both couples of operators (see Fig. 11 obtained with the BS couple).

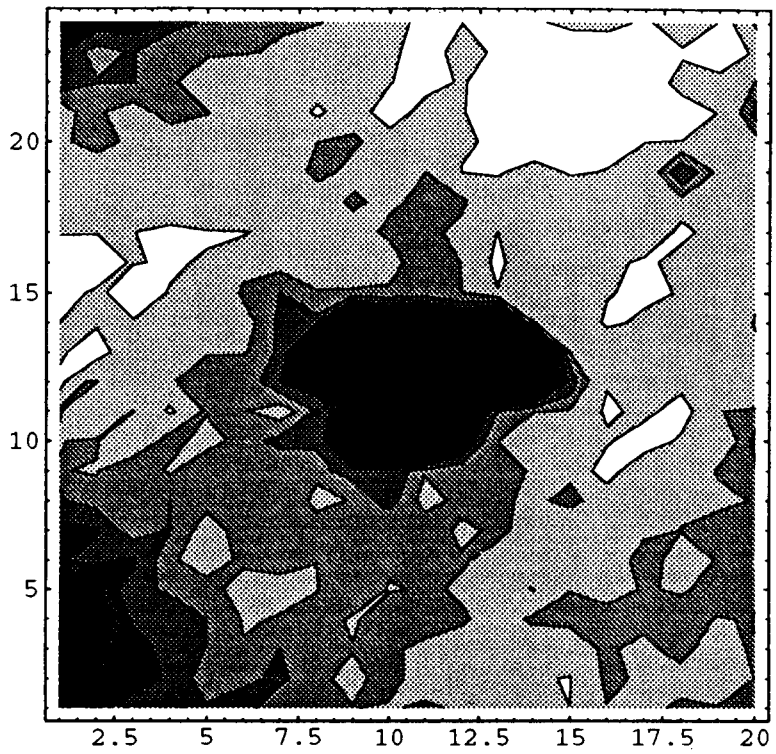


Fig. 12. Enlarged view from Eq. (19) and BS operators.

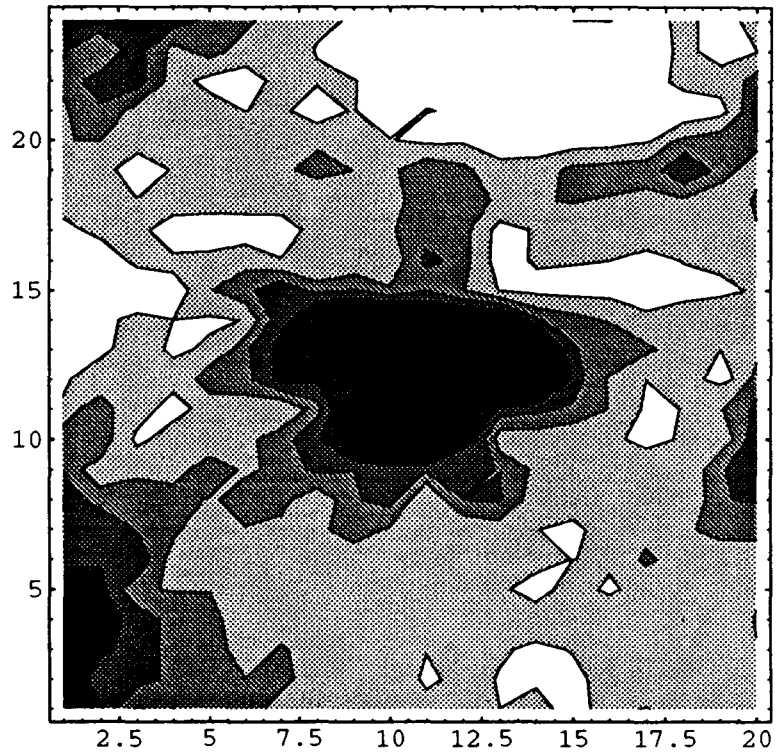


Fig. 13. Enlarged view from Eq. (19) and AP operators.

Similar conclusions can be drawn by observing the three enlarged views of the region containing the central obstacle, shown, respectively, in Figs. 12–14 in the same order as before. In particular, in the first density plot the obstacle appears very well outlined and sufficiently separated from the wall.

## 6. Conclusions

A new approach is proposed to build maps for autonomous mobile robots. Fuzzy set theory has been successfully used to manage the uncertainties resulting from the characteristics of typical sensors. Moreover, it allows to describe, in a very natural way, the operations necessary to extract specific types of information from the maps.

A prototype system has been realized in our laboratory, using the well-known Polaroid ultrasonic sensors. It has been successfully tested and has shown the advantages of the described approach. The quality of the obtained maps is noteworthy, in particular if compared with that of other maps presented in the literature.

The proposed structure can be also used to include information deriving from different kinds of devices. As a matter of fact, only the modeling of the uncertainties they introduce is required. Also incremental map building, typical of robots navigating in an unknown environment, can be easily allocated in the proposed framework. The use of a NOMAD 200 mobile unit is providing the way to test the approach in a real case. Further researches in our laboratory include the search of an "optimal" path on a fuzzy map. This is an intriguing problem as the usual definitions of optimality, e.g. the shortest path, are difficult to apply in presence of uncertainty, as in the case of sensor-based reconstruction of the environment. New methods are

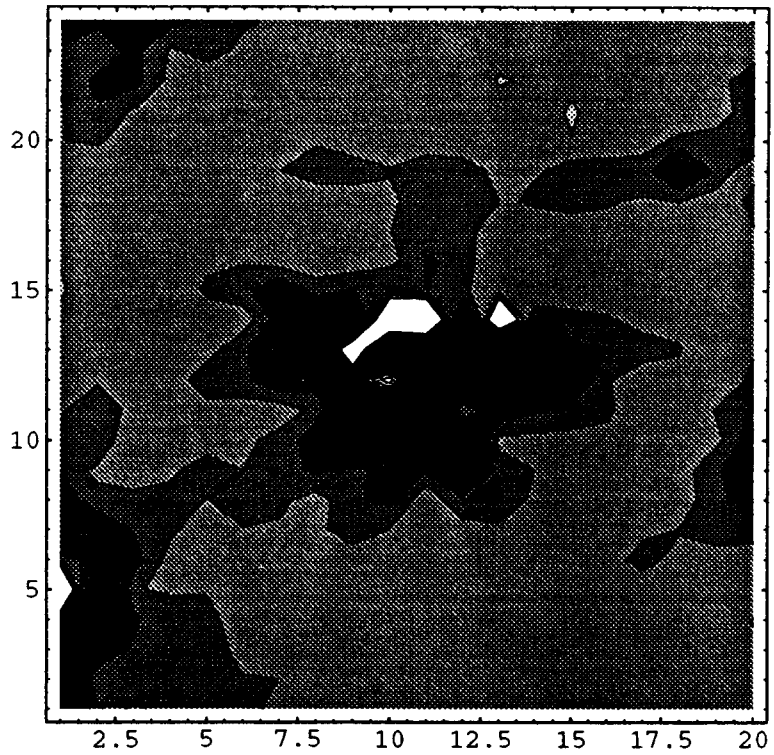


Fig. 14. Enlarged view from Eq. (18) and BS operators.

required: a viable possibility is a trade-off between length and risk; this again calls for a fuzzy approach. Among the algorithms under investigations there are both graph-searching (e.g. $A^*$) and potential based ones.

## Acknowledgments

This work has been partially supported by M.U.R.S.T. 40% funds.

## References

[1] H. Bandemer and W. Nather, *Fuzzy Data Analysis* (Kluwer Academic Publishers, Dordrecht, 1992).
[2] I.J. Cox and G.T. Wilfong, *Autonomous Robot Vehicles* (Springer, Berlin, 1990).
[3] J. Dombi, A general class of fuzzy operators, the de morgan class of fuzzy operators and fuzziness measure induced by fuzzy operators, *Fuzzy Sets and Systems* **8** (1982).
[4] H.F. Durrant-Whyte, *Integration Coordination and Control of Multi-sensor Robot Systems*, Vol. SECS 36, *International Series in Engineering and Computer Science* (Kluwer Academic Publishers, Norwell, MA, 1988).
[5] A. Elfes and H.P. Moravec, High resolution maps from wide angle sonar, *IEEE Internat. Conf. on Robotics and Automation*, St. Louis, MO, (1985) pp. 116–121.
[6] G.D. Hager, *Task-Directed Sensor Fusion and Planning: A Computational Approach*, Vol. SECS 99, *International Series in Engineering and Computer Science* (Kluwer Academic Publishers, Norwell, MA, 1990).
[7] J. Hwan, L. Dong and W. Cho, Physically based sensor modeling for a sonar map in a specular environment, *IEEE Internat. Conf. on Robotics and Automation*, Nice, France (1992) pp. 1714–1719.

[8] J.M. Keller and R. Krishnapuram, Fuzzy sets methods in computer vision, in: R. Yager and L.A. Zadeh, Eds., *An Introduction to Fuzzy Logic Applications in Intelligent Systems* (Kluwer Academic Publishers, Dordrecht, 1992).
[9] A. Kemurdjian, V. Granov and U. Mishkinyuk, Small marsokhod configuration, *IEEE Internat. Conf. on Robotics and Automation* Nice, France (1992) pp. 165–168.
[10] G.J. Klir and T.A. Folger, *Fuzzy Sets, Uncertainty and Information* (Prentice-Hall, Englewood Cliffs, NJ, 1988).
[11] E. Krotkov and R. Simmons, Performance of a six-legged planetary rover: Power, positioning and autonomous walking, *IEEE Internat. Conf. on Robotics and Automation*, Nice, France (1992) pp. 169–174.
[12] R. Kuc and M.W. Siegel, Physically based simulation model for acoustic sensor robot navigation, *IEEE Trans. Pattern Analysis Machine Intelligence* **PAMI-9**(6) (1987) 766–778.
[13] Y. Maeda et al., Hierarchical control for autonomous mobile robots with behaviour decision fuzzy algorithm, *IEEE Internat. Conf. on Robotics and Automation*, Nice, France (1992).
[14] C. Pal and J. Bezdek, *Fuzzy Models for Pattern Recognition* (IEEE Press, New York, 1991).
[15] S.K. Pal, Fuzziness, image information and scene analysis, in: R. Yager and L.A. Zadeh, Eds., *An Introduction to Fuzzy Logic Applications in Intelligent Systems* (Kluwer Academic Publishers, Dordrecht, 1992).
[16] Polaroid Corporation, *Polaroid Ultrasonic Ranging System Handbook Application Notes/Technical Papers.*
[17] Polaroid Corporation, *Ultrasonic Ranging System.*
[18] F.G. Pin and H. Watanabe et al., Autonomous navigation of a mobile robot using custom designed qualitative reasoning vlsi chips, *IEEE Internat. Conf. on Robotics and Automation*, Nice, France (1992).
[19] H. Prade and D. Dubois, A review of fuzzy set aggregation connectives, *Inform. Sci.* **36** (1985).
[20] A. Pruski and C. Bourkis, The vahm project: a cooperation between an autonomous mobile platform and a disabled person, *IEEE Internat. Conf. on Robotics and Automation*, Nice, France (1992).
[21] B. Wilcox and L. Matthies et al., Robotic vehicles for planetary exploration, *IEEE Internat. Conf. on Robotics and Automation*, Nice, France (1992) pp. 175–180.
[22] R.R. Yager, On a general class of fuzzy connectives, *Internat. J. Fuzzy Sets and Systems* **4** (1980).
[23] H.J. Zimmermann, *Fuzzy Set Theory and Its Applications* (Kluwer Academic Publishers, Dordrecht, 1991).